Received: 9 April 2019 | Revised: 29 November 2019 | Accepted: 3 December 2019

DOI: 10.1002/navi.356

ORIGINAL ARTICLE

WILEY ION

Galileo model of group delay accuracy for advanced RAIM users

Ilaria Martini[1] | **Matteo Sgammini**[2] | **Juan Pablo Boyero**[3]

[1]European Commission Advisor, Rhea, Brussels, Belgium

[2]European Commission, Joint Research Center (JRC),Ispra, Italy

[3]European Commission Directorate General,Defence Industry and Space, Brussels, Belgium

Correspondence
Ilaria Martini, European Commission, Rhea, Brussels, Belgium.
Email: i.martini@rheagroup.com

Present Address
Avenue Pasteur 23, 1300 Brussels, Belgium

Abstract

Group delays (GDs) are errors affecting Global Navigation Satellite Systems (GNSS) due to non-idealities of the satellite or the receiver hardware and can compromise safety critical applications (eg, advanced receiver autonomous integrity monitoring [ARAIM]) when integrity requirements are at major or even hazardous safety level. The paper shows that GPS uses L1 and L2 signals in the generation of the navigation message, and as a consequence, an L1-L5 dual-frequency user must include the GD contribution in the integrity assessment. For Galileo, whose navigation message refers to the aviation frequencies (E1 and E5), the GDs can be modeled separately from the Signal In Space Accuracy (SISA), because they affect only single-frequency users. This model permits a reduction of User Ranging Accuracy (URA) values with respect to those of GPS, thus improving availability for dual-frequency users. Characterizing the GD of Galileo navigation messages, the paper describes a method to include the GD error model in ARAIM and its potential advantages.

1 | INTRODUCTION

Group delays (GDs) affect ranging measurements and represent differences between the actual measurement and an ideal observation. There are several contributors to these errors, each of them not always easy to identify and separate.

Satellite signal distortions can be digital or analogue,[1] and in the latter case, in particular, the receiver and satellite contributions are highly correlated, due to the non-linearity of the processes involved.[2] The effect of the receiver GD depends on its characteristics, like the bandwidth and the correlator spacing. The antenna contribution varies with its characteristics, for example, its anisotropy,[3] and only a characterization performed in a laboratory can properly parse out this contribution. Although these effects are assumed negligible in many Global Navigation Satellite Systems (GNSS) applications, in the context of safety of life services, GDs, especially satellite contributions, should be properly modeled and taken into account by aviation single-frequency (SF) users.

Constellation Service Providers (CSPs) broadcast parameters in the navigation message to partially correct the satellite contribution to the GD. These errors have been extensively assessed and characterized in the literature,[4-7] but the focus has been mostly on the User Ranging Accuracy (URA).

For safety critical applications, the integrity level requires not only a high accuracy of the ranging but also a proper bounding of the residual ranging errors. It is particularly important to ensure that the probabilities of rare ranging outliers are properly modeled when computing the so-called protection level. This is of primary importance, for example, for aviation users.

The International Civil Aviation Organization (ICAO) and the entities responsible for standards setting, such as the Radio Technical Commission for Aeronautics (RTCA) and European Organisation for Civil Aviation Equipment (EUROCAE), are developing aviation standards for Dual Frequency Multi-Constellation services (DFMC), which

covers the use of the multiconstellation satellite–based augmentation system (SBAS), dual-frequency (DF), and SF advanced receiver autonomous integrity monitoring (RAIM).[8]

The current aviation reference document, Minimum Operational Performance Standard (MOPS DO-229[9]), provides the "standard for single frequency airborne navigation" in particular for L1 users. The extension of the standard to dual-frequency L1-L5 and SF L5 users would require a proper treatment of the GD contribution. In this paper, we address the open question on how the SF MOPS DO-229 GD models need to be modified for the new DFMC MOPS.

GPS and Galileo present several differences on this aspect. Among others, the main one is related to the generation of the navigation message. As heritage of its long history, GPS ground monitoring uses L1 and L2 measurements to generate the navigation message, while Galileo uses E1 and E5 messages. This means that in contrast to GPS, Galileo processes the same signals used by aviation users. For GPS instead, the conversion of broadcast parameters from L1-L2 to L1-L5 is performed by the user applying the broadcast GDs (BGDs). These parameters need to be applied not only by SF but also by L1-L5 dual-frequency users. This is not the case for Galileo, whose E1-E5 users are not affected by these terms.

The consequence is that the treatment of delays among different signals can be simplified in the Galileo user case compared with that of GPS. For the latter, URA must include the residual GD errors for both SF (L1 and L5) and dual-frequency (L1-L5) users, while for Galileo, the residual GD errors must be accounted only for SF users (E1 and E5).

Thus, Galileo can model separately the two contributions using two different terms: one for the GD bound and one for the DF URA. This allows a reduction of the URA term improving availability for DF advanced receiver autonomous integrity monitoring (ARAIM) users. Furthermore, the GD term is expected to be negligible with respect to the other SF contributions, such as the ionospheric residual error[10]: margins can be taken to properly accommodate outliers.

This paper presents a novel model of URA and BGD bounding for Galileo. The advantages of this model are described in this paper, and resulting bounding values are provided and validated through a measurement campaign. Since ARAIM users will use GPS in combination with Galileo, a characterization of the GPS GD accuracy is also included to complete the analysis of ARAIM SF users. This allows us to show the advantages of the proposed method with respect to the GPS methods used in the MOPS DO-229.

The first section of this paper provides a general formulation of GNSS GDs affecting dual-frequency and SF users. Section 2 focuses on the GPS and Galileo cases, describing the information that is broadcast in the navigation message to correct the GDs. Section 3 analyzes the URA bounding for GPS and Galileo and how each affects GD accuracy. Finally, Section 4 presents the novel model of the GD accuracy for Galileo with justification based on real measurements. Section 4 also provides preliminary values of the GD bounds to support the definition of the aviation (DFMC MOPS) and Galileo standards.[11]

2 | GENERAL MODEL OF RANGING GDS

Since the magnitude of GD biases cannot be directly measured on the ground, as only the difference between the two signals can be observed, CSPs define the BGDs as the difference between a ranging measurement and a reference signal. These biases are then generally modeled and treated as differential GDs (DGDs).

In addition, CSPs transmit corrections for the DGD within the navigation message. Not all possible combinations are provided but only those for a certain set of signals. The user reconstructs the GD referring to its specific signal by applying some simple processing.

This section presents the generic formulation of the ranging bias for single and dual-frequency users as function of the BGDs. These formulations are valid for all GNSS signals. The following sections focus on Galileo and GPS cases.

The pseudorange measured on the line of sight between a satellite i and a receiver j and on a generic signal s is

$$\rho_s^{i,j} = \left\| x^j - x^i \right\| + \tau^j - \tau^i + T^{i,j} + I_s^{i,j} + \epsilon_s^{i,j} + B_s^i + B_s^j \quad (1)$$

where x^j and x^i are respectively the receiver and satellite positions in Earth Centered Earth Fixed (ECEF) coordinate system; τ^j and τ^i are respectively the receiver and satellite clock errors (m); $T^{i,j}$ is the tropospheric error (m); $I_s^{i,j}$ is the ionospheric error of the signal s (m); and $\epsilon_s^{i,j}$ is the receiver noise including thermal and local effects (m).

The term B_s represents the measurement delay due to systematic differences between the actual measurement and an ideal observation, free of signal distortions, antenna phase delay, satellite hardware GDs, and analogous receiver ranging errors. The major components of this term are thus originated from hardware-related delays in the receiver front-end (B_s^j) and in the satellite payload (B_s^i).

Ranging delays are dependent on the receiver, the satellite, and the signal s. In particular, not only the frequency impacts on the GD but also characteristics like the modulation and the chip rate affect this term. This means

that different signal components at the same frequency can produce in principle different delays.

As specified in the GPS standard paragraph 3.3.1.7[12]), equipment GD is defined as the delay between the signal radiated output of a specific satellite (SV) (measured at the antenna phase center) and the output of that satellite on-board frequency source.

The receiver contribution B_s^j can be neglected since it is absorbed in the receiver clock offset and will not be included in the following equations.

The ionosphere-free measurement obtained combining pseudoranges (1) on two generic signals, $s1$ and $s2$, is

$$\rho^{i,j}_{IF(s1,s2)} = \left\| x^j - x^i \right\| + \tau^j - \tau^i + T^{i,j} + \epsilon^{i,j}_{IF(s1,s2)} + \frac{f_{s1}^2}{(f_{s1}^2 - f_{s2}^2)} \cdot B^i_{s1} - \frac{f_{s2}^2}{(f_{s1}^2 - f_{s2}^2)} \cdot B^i_{s2} \tag{2}$$

and contains a combination of the absolute signal delays scaled by frequency-dependent factors.

The next two sections detail the formulation of the GD for dual-frequency and SF users.

2.1 | GDs for dual-frequency users

CSPs use a convention that simplifies the processing for dual-frequency users. Included in the broadcast satellite clock offset, τ^i, is in fact the satellite GD contribution, $\frac{f_{s1}^2}{(f_{s1}^2-f_{s2}^2)} \cdot B^i_{s1} - \frac{f_{s2}^2}{(f_{s1}^2-f_{s2}^2)} \cdot B^i_{s2}$.

This means that the broadcast clock parameters correct the following dual-frequency clock error:

$$\tau^i_{IF(s1,s2)} = \tau^i - \frac{f_{s1}^2}{(f_{s1}^2 - f_{s2}^2)} \cdot B^i_{s1} + \frac{f_{s2}^2}{(f_{s1}^2 - f_{s2}^2)} \cdot B^i_{s2}. \tag{3}$$

The CSP convention simplifies the processing for dual-frequency users, in which case there is no need to apply any BGD. A dual-frequency pseudorange has in fact the following expression:

$$\rho^{i,j}_{IF(s1,s2)} = \left\| x^j - x^i \right\| + \tau^j - \tau^i_{IF(s1,s2)} + T^{i,j} + \epsilon^{i,j}_{IF(s1,s2)}. \tag{4}$$

It is important to point out that this simplification is actually applicable only for users that combine the same signals, $s1$ and $s2$, which are used by the CSP as reference for the navigation message. A generic dual-frequency user combining a pair of different signals, $s3$ and $s4$, is instead characterized by the following ranging equation:

$$\rho^{i,j}_{IF(s3,s4)} = \left\| x^j - x^i \right\| + \tau^j - \tau^i + T^{i,j} + \epsilon^{i,j}_{IF(s3,s4)} + \frac{f_{s3}^2}{(f_{s3}^2 - f_{s4}^2)} \cdot B^i_{s3} - \frac{f_{s4}^2}{(f_{s3}^2 - f_{s4}^2)} \cdot B^i_{s4}. \tag{5}$$

After applying the broadcast clock parameters (3), the user is affected by the following bias:

$$B^i_{IF(s3,s4)} = \frac{f_{s1}^2}{(f_{s1}^2 - f_{s2}^2)} \cdot B^i_{s1} - \frac{f_{s2}^2}{(f_{s1}^2 - f_{s2}^2)} \cdot B^i_{s2} + \frac{f_{s3}^2}{(f_{s3}^2 - f_{s4}^2)} \cdot B^i_{s3} - \frac{f_{s4}^2}{(f_{s3}^2 - f_{s4}^2)} \cdot B^i_{s4}. \tag{6}$$

In the intermediate case, when the user processes only one of the reference signals, $s1$ and $s2$, the bias is simplified. For example, a $s3$ and $s1$ ionosphere-free pseudorange combination would be affected by the following delay:

$$B^i_{IF(s3,s1)} = \frac{f_{s1}^2}{(f_{s1}^2 - f_{s2}^2)} \cdot B^i_{s1} - \frac{f_{s2}^2}{(f_{s1}^2 - f_{s2}^2)} \cdot B^i_{s2} + \frac{f_{s3}^2}{(f_{s3}^2 - f_{s1}^2)} \cdot B^i_{s3} - \frac{f_{s1}^2}{(f_{s3}^2 - f_{s1}^2)} \cdot B^i_{s1}. \tag{7}$$

All other combinations can be derived similarly from Equation (6).

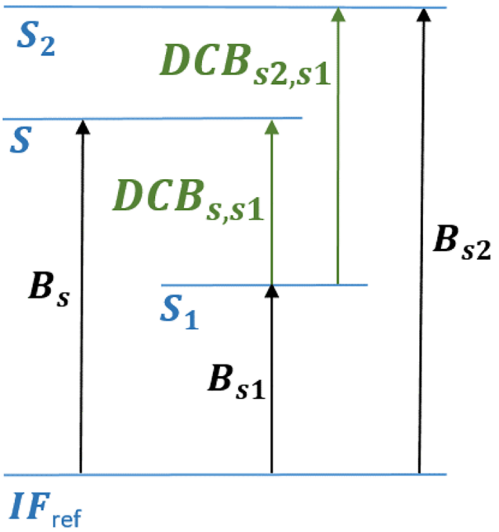

FIGURE 1 Diagram illustrating the relationship of group delays between signals and ionosphere-free combinations. Broadcast navigation messages of GPS and Galileo refer to ionosphere-free combination (IF_{ref}). Single-frequency users need to apply broadcast group delay to the IF_{ref} clock offset. In both the figure and text description, $s1$ and $s2$ indicate the signals used as reference for the navigation message, while s indicates a generic signal different from them [Color figure can be viewed at wileyonlinelibrary.com and www.ion.org]

2.2 | GDs for SF users

An SF user measuring a third signal, s, is also affected by GDs described by the following expression:

$$\rho_s^{i,j} = \left\| x^j - x^i \right\| + \tau^j - \tau^i_{IF(s1,s2)} + T^{i,j} + I_s^{i,j} + \epsilon_s^{i,j} + B_s^i - B_{s1}^i + \frac{f_{s2}^2}{(f_{s1}^2 - f_{s2}^2)} \cdot \left(B_{s2}^i - B_{s1}^i\right). \quad (8)$$

If the signal s is instead one of the two reference signals, $s1$ or $s2$, the biases are described in the CSP Interface Control Document.[11-13] In these cases, the user has to apply a simple scaling factor to the BGD:

$$B_{s1}^i = \frac{f_{s2}^2}{(f_{s1}^2 - f_{s2}^2)} \cdot \left(B_{s2}^i - B_{s1}^i\right), \quad (9)$$

$$B_{s2}^i = \frac{f_{s1}^2}{(f_{s1}^2 - f_{s2}^2)} \cdot \left(B_{s2}^i - B_{s1}^i\right) \quad (10)$$

The differences of GDs between two signals are usually named DGD or differential code biases (DCBs) (Equations (9) and (10)). Figure 1 shows the GD relationship between the two reference signals of the navigation message, $s1$ and $s2$, the ionosphere-free combination, IF_{ref}, and a generic signal, s.

To this point, the GD formulation for a generic user has been described and discussed. Formulae are much simpler when considering the specific cases of GPS and Galileo, as described in the next section.

3 | GPS AND GALILEO GD BROADCAST IN THE NAVIGATION MESSAGES

This section describes the use of the GD information provided by GPS and Galileo through the Signal In Space navigation message.

This paper focuses in particular on aviation services. The L2 signal is not considered, since this frequency is not in the bandwidth allocated to aviation users by the International Telecommunication Union (ITU). Nevertheless, the concepts presented in the paper are applicable to all services based on Galileo signals.

3.1 | GPS case

This section contains a description of DGD corrections provided by GPS in the broadcast navigation message. An overview of the GPS signal components for each frequency is provided in the Rinex Format Definition Document[14] (Table 1). Note that the IGS Rinex naming convention used

TABLE 1 GPS signals components and characteristics as described in Rinex Format Definition Document[14]

GNSS System	Freq. Band /Frequency	Channel or Code	Observation Codes Pseu Range	Carrier Phase	Doppler	Signal Strength
GPS	L1/1575.42	C/A	C1C	L1C	D1C	S1C
		L1C(D)	C1S	L1S	D1S	S1S
		L1C(P)	C1L	L1L	D1L	S1L
		L1C(D+P)	C1X	L1X	D1X	S1X
		P(AS off)	C1P	L1P	DIP	S1P
		Z-tracking and similar (AS on)	C1W	L1W	D1W	S1W
		Y	C1Y	L1Y	D1Y	S1Y
		M	C1M	L1M	D1M	S1M
		Codeless		L1N	D1N	S1N
	L2/1227.60	C/A	C2C	L2C	D2C	S2C
		L1(C/A)+(P2-P1) (semi-codeless)	C2D	L2D	D2D	S2D
		L2C(M)	C2S	L2S	D2S	S2S
		L2C(L)	C2L	L2L	D2L	S2L
		L2C(M+L)	C2X	L2X	D2X	S2X
		P(AS off)	C2P	L2P	D2P	S2P
		Z-tracking and similar (AS on)	C2W	L2W	D2W	S2W
		Y	C2Y	L2Y	D2Y	S2Y
		M	C2M	L2M	D2M	S2M
		Codeless		L2N	D2N	S2N
	L5/1176.45	I	C5I	L5I	D5I	S5I
		Q	C5Q	L5Q	D5Q	S5Q
		I+Q	C5X	L5X	D5X	S5X

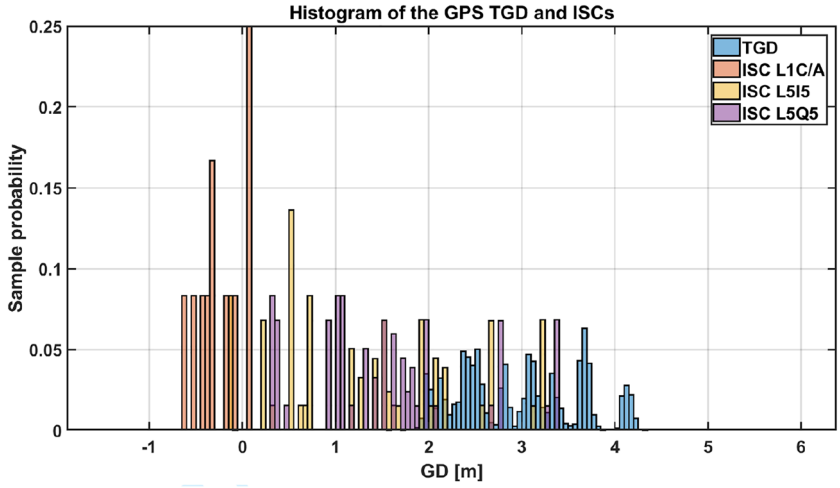

FIGURE 2 Histogram of GPS TGDs and ISCs broadcast between 01/02/2017 and 01/03/2018 [Color figure can be viewed at wileyonlinelibrary.com and www.ion.org]

in the table can differ from that used by GPS and Galileo standards.

Table 1 contains the full list of GPS signals and shows that there are several GDs, one for each different signal component. In fact, each entry of the third column has different signal characteristics and has in principle a different GD.

In the GPS standards,[12,13] the description of the broadcast DGD corrections specifies that the navigation message refers to L1P(Y) and L2P(Y) signals:

> *Since the SV clock corrections are estimated by the CSP using dual frequency L1P(Y) and L2P(Y) code measurements, the single-frequency L1, L2 or L5 user and dual frequency L1 C/A-L2C, L1 and L5, L2 and L5 must apply additional terms.*

These terms are the inter-signal corrections (ISCs) transmitted in the Civil Navigation (CNAV) message and the time GD (TGD) transmitted in the CNAV and Legacy Navigation (LNAV) messages (paragraph 30.3.3.3.1.1.[12]).

It is highlighted that GPS standards also specify that dual-frequency users need to apply DGDs as SF users do.

This contribution is also not negligible in the ranging error budget, as indicated in paragraph 3.3.1.7.2[13]:

> *For a given navigation payload redundancy configuration, the absolute value of the mean differential delay shall not exceed 30.0 nanoseconds.*

Measurements from real Signal In Space confirm this range of values, as shown in Figure 2. The delays in this case are converted from seconds to meters by multiplying them by the speed of light.

For this analysis, MGEX IGS Rinex files in an experimental format containing CNAV messages (brdx) have been used.[15] In these files, TGD and ISCs of CNAV GPS SIS were extracted and combined to assess the GDs. The IGS webserver used was ftp://ftp.cddis.eosdis.nasa.gov/gnss/data/campaign/mgex/daily/rinex3/.

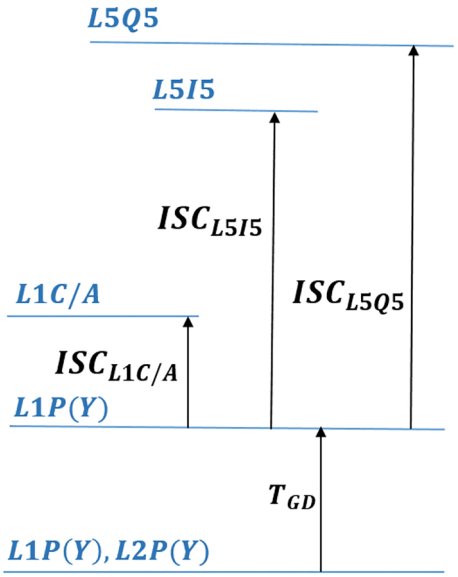

FIGURE 3 Relationship between time group delay (TGD) and inter-signal corrections (ISCs) on L1 and L5 signals, showing construction of the offsets to be added to the broadcast clock offset by GPS single-frequency users [Color figure can be viewed at wileyonlinelibrary.com and www.ion.org]

It can be observed that DGD values can reach the 4.50 m value specified in the standard.[12]

The user combines the broadcast parameters shown in Figure 2 and reconstructs the corrections to be applied to the dual-frequency satellite clock offset, as specified in paragraph 20.3.3.3.3.2[12]

> *the user who utilizes the L1P(Y) signal only shall modify the code phase offset in accordance with paragraph 20.3.3.3.3.1 with the*

equation:

$$\tau^i_{L1P(Y)} = \tau^i_{L1P(Y),L2P(Y)} - T_{GD}. \quad (11)$$

An L1C/A SF user needs to apply the broadcast TGD and ISC terms in paragraph 30.3.3.3.1.1.1[12]:

$$\tau^i_{L1C/A} = \tau^i_{L1P(Y),L2P(Y)} - T_{GD} + ISC_{L1C/A}. \quad (12)$$

The L1P(Y) and L1C/A contributions can also be derived from Equation (9) presented in the previous section, while L5I and L5Q SF users must instead apply the following corrections (paragraph 20.3.3.3.1.2.1[13]):

$$\tau^i_{L5I} = \tau^i_{L1P(Y),L2P(Y)} - T_{GD} + ISC_{L5I5}, \quad (13)$$

$$\tau^i_{L5Q} = \tau^i_{L1P(Y),L2P(Y)} - T_{GD} + ISC_{L5Q5}. \quad (14)$$

Figure 3 shows the relationship between GPS broadcast DGD and SF clock corrections as described in paragraph 20.3.3.3.3.[12]

While a GPS L1P(Y)-L2P(Y) user would not need to apply any DGD terms, other users (ie, L1C/A-L2P(Y) or L1C/A-L2C/A or L1C/A-L5Q5) must apply GD corrections. In particular, an aviation L1-L5 user must add the term specified in paragraph 20.3.3.3.1.2.2[13] corresponding to Equation (7). This corresponds to the following GPS

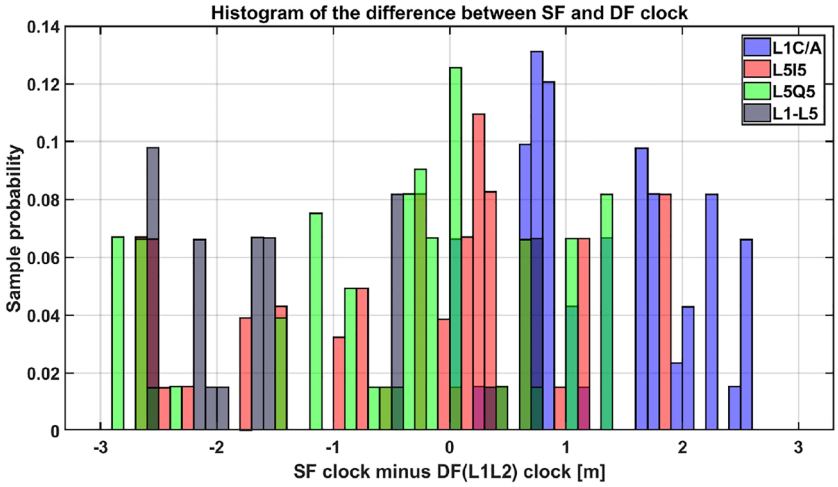

FIGURE 4 Histogram of DGD contribution to GPS L1P(Y)-L2P(Y) clock for L1C/A, L5I5, and L1C/A-L5I5 users between 01/02/2017 and 01/03/2018 [Color figure can be viewed at wileyonlinelibrary.com and www.ion.org]

TABLE 2 Galileo signals components and characteristics as described in Rinex Format Definition Document[14]

GNSS System	Freq. Band /Frequency	Channel or Code	Observation Codes Pseu Range	Carrier Phase	Doppler	Signal Strength
Galileo	E1/1575.42	A PRS	C1A	L1A	D1A	S1A
		BI/NAV OS/CS/SoL	C1B	L1B	D1B	S1B
		C no data	C1C	L1C	D1C	S1C
		B+C	C1X	L1X	D1X	S1X
		A+B+C	C1Z	L1Z	D1Z	S1Z
	E5a/1176.45	IF/NAV OS	C5I	L5I	D5I	S5I
		Q no data	C5Q	L5Q	D5Q	S5Q
		I+Q	C5X	L5X	D5X	S5X
	E5b/1207.140	II/NAV OS/CS/Sol	C7I	L7I	D7I	S7I
		Q no data	C7Q	L7Q	D7Q	S7Q
		I+Q	C7X	L7X	D7X	S7X
	E5(E5a+E5b)/ 1191.795	I	C8I	L8I	D8I	S8I
		Q	C8Q	L8Q	D8Q	S8Q
		I+Q	C8X	L8X	D8X	S8X
	E6/1278.75	A PRS	C6A	L6A	D6A	S6A
		BC/NAV CS	C6B	L6B	D6B	S6B
		C no data	C6C	L6C	D6C	S6C
		B+C	C6X	L6X	D6X	S6X
		A+B+C	C6Z	L6Z	D6Z	S6Z

L1L5 clock offset:

$$\tau^i_{L1L5I} = \tau^i_{L1P(Y),L2P(Y)} - T_{GD} + \frac{ISC_{L5I5} - \Upsilon_{L1L5} \cdot ISC_{L1C/A}}{1 - \Upsilon_{L1L5}}, \quad (15)$$

$$\tau^i_{L1L5Q} = \tau^i_{L1P(Y),L2P(Y)} - T_{GD} + \frac{ISC_{L5Q5} - \Upsilon_{L1L5} \cdot ISC_{L1C/A}}{1 - \Upsilon_{L1L5}}, \quad (16)$$

where $\Upsilon_{L1L5} = \frac{f^2_{L1}}{f^2_{L5}}$.

Figure 4 shows statistics of the GPS clock corrections for both SF L1C/A, L5I5, and L5Q5 and dual-frequency L1C/A-L5I5 users. Note that the DGDs are uniformly distributed in the range of −3 to 3 m with no single component dominating the others and confirming the range specified in the GPS standard.

3.2 | Galileo case

For Galileo, the positioning services are defined on two types of navigation messages, FNAV on E1-E5a and INAV on E1-E5b signals. This implies that two types of dual-frequency users do not need to apply DGD corrections (Equation (4)).

Table 2 shows the full set of Galileo signals as reported in the Rinex Format Definition Document.[14]

Figure 5 shows the BGD in the FNAV message transmitted on the E5a signal for Galileo satellites over one day (10/02/2017). Except for satellite GSAT (PRN E24), whose BGD corrects satellite hardware delays caused by the on-board clock characteristics, BGD differences among satellites are on the order of 6 m. BGDs are usually stable over time and are updated daily around noon (in Galileo System Time for which the offset from UTC is below 30 ns, 95% of the time[16]). Variations between consecutive updates are generally on the order of tens of centimeters.

In the Galileo case, the contribution of the DGD to the satellite clock error for an E5a SF user is shown in Figure 5. For the E1 SF case, the clock offset is equal to the BGD in the INAV message (Figure 6) without the need to apply any scaling factors as indicated in Equations (9) and (10).

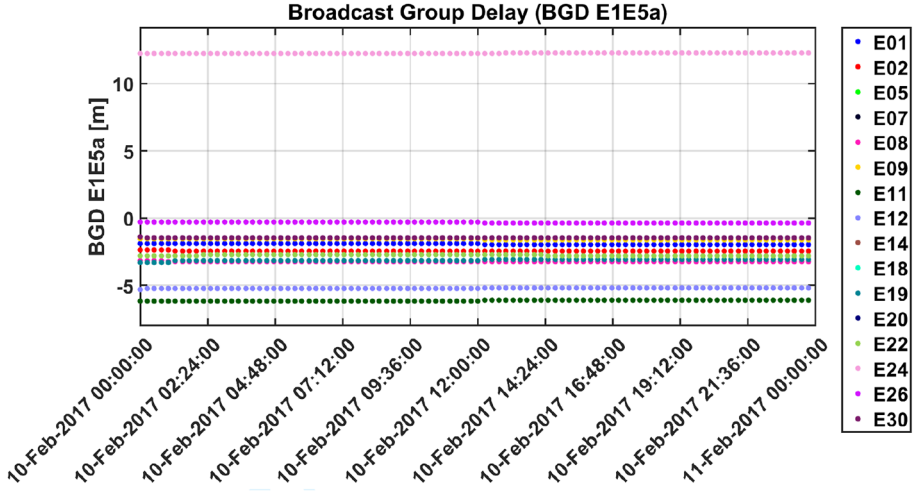

FIGURE 5 Time series of Galileo broadcast group delay on E1-E5a [Color figure can be viewed at wileyonlinelibrary.com and www.ion.org]

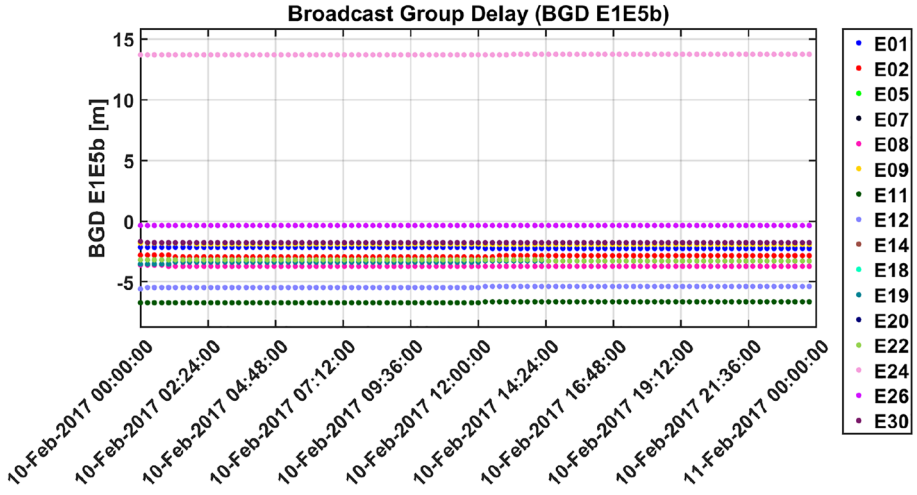

FIGURE 6 Time series of Galileo broadcast group delay on E1-E5b [Color figure can be viewed at wileyonlinelibrary.com and www.ion.org]

4 | ACCURACY OF BROADCAST GROUP DELAYS

This section focuses on the GD residual error after applying the broadcast corrections described in the previous sections. In particular, it focuses on the URA broadcast in the GPS and Galileo navigation messages, these being the terms bounding the residual errors that contribute to the integrity performance. The DGD residual errors must be correctly modeled because they affect the user integrity and the protection level computation.

This section presents a characterization of the DGD accuracy, which has been performed comparing IGS-MGEX DCB[15] with broadcast data from 01/01/2018 till 01/09/2018 as described in reference papers.[5,6] GPS IIF satellites messages were analyzed to characterize L5 signals. In particular, the DCBs provided by IGS were selected and compared to the broadcast parameters multiplied by the speed of light c according to the following relationships:

$$c \cdot TGD = -\frac{f_{L1}^2}{f_{L1}^2 - f_{L2}^2} \cdot DCB_{C1W-C2W}, \quad (17)$$

$$c \cdot ISC_{L1C/A} = -DCB_{C1C-C1W}, \quad (18)$$

$$c \cdot ISC_{L5I5} = -DCB_{C5I-C1W}, \quad (19)$$

$$c \cdot ISC_{L5Q5} = -DCB_{C5Q-C1W}, \quad (20)$$

$$c \cdot BGD_{E1-E5a} = -\frac{f_{E1}^2}{f_{E1}^2 - f_{E5}^2} \cdot DCB_{C1B-C5I}, \quad (21)$$

$$c \cdot BGD_{E1-E5b} = -\frac{f_{E1}^2}{f_{E1}^2 - f_{E5}^2} \cdot DCB_{C1B-C7I}. \quad (22)$$

4.1 | GPS case

As reported in the GPS standard (paragraph 3.3.1.7.2[12]):

> *The random plus non-random variations about the mean shall not exceed 3.0 nanoseconds (95% probability), when including consideration of the temperature and antenna effects during a vehicle orbital revolution.*

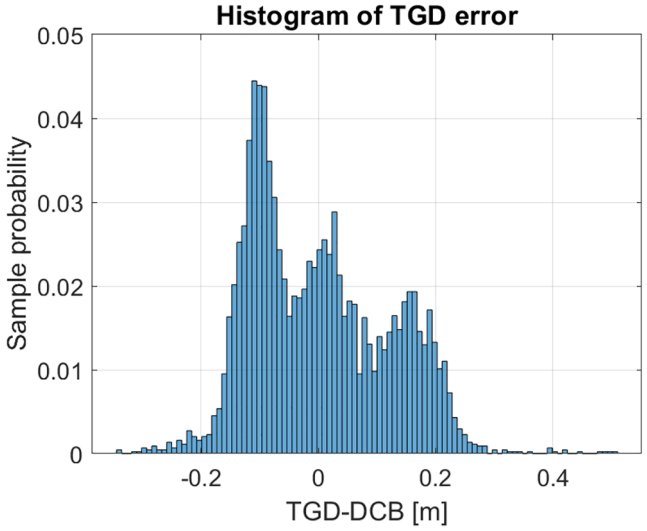

FIGURE 8 Histogram of GPS time group delay (TGD) error for L1P(Y) users with respect to L1P(Y)-L2P(Y) users [Color figure can be viewed at wileyonlinelibrary.com and www.ion.org]

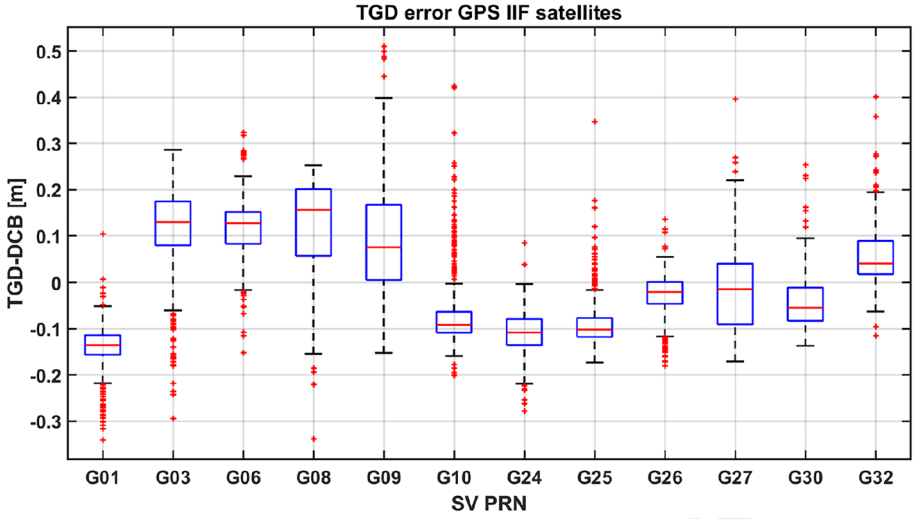

FIGURE 7 Box plot of GPS time group delay (TGD) error affecting L1P(Y) users with respect to L1P(Y)-L2P(Y) users (Equation (11)). On each box, the central mark indicates the median, and the bottom and top edges of the box indicate the 25th and 75th percentiles, respectively. The whiskers extend to the most extreme data points not considered outliers, and the outliers are plotted individually using the "+" symbol. The boxplot draws points as outliers if they are greater than $q3 + 2.7\sigma \times (q3 - q1)$ or less than $q1 - 2.7\sigma \times (q3 - q1)$, where $q1$ and $q3$ are the 25th and 75th percentiles of the sample data, respectively, and σ sample standard deviation [Color figure can be viewed at wileyonlinelibrary.com and www.ion.org]

The GPS standard indicates an upper bound of 90 cm for the errors in the DGD values. The measurement campaign performed in this study confirmed this upper bound.

Figure 7 shows the box plot of the error on the TGD for each GPS satellite (Equation (17)). Comparing the results of Figure 7 (per satellite) with those of Figure 8 (for the whole constellation), it is observed that the mean value for each satellite differs from the others up to several centimeters but over the whole constellation, the distribution is averaged around zero (although not quite symmetric).

Previous results focused on the accuracy of the single broadcast TGD. Now, by analyzing the accuracy of the clock offset obtained by combining TGDs and ISCs (as described in Figure 3 and Equations (11) and (16)), the contribution to the URA bound is obtained in Figure 9.

It is important to highlight that GPS L1-L5 dual-frequency users are also affected by DGD errors, with this contribution (in gray) being the largest, even larger than those of the SF cases (Figure 9). This means that the GPS URA bound is driven by the DF L1-L5 user case and needs to be inflated due to the DGD inaccuracies.

Equation (15) shows that the GPS DF clock includes more terms (TGD and two ISCs) and their inaccuracies summed in the overall URA bound.

4.2 | Galileo case

In the Galileo case, the DGD accuracy is on the same order of magnitude as the GPS case, and the clock contribution is just a scaled version of the BGD value.[11] Figures 10 and 11 show the errors respectively on each satellite and the statistic aggregating all satellites. Results were obtained applying Equation (21). A similar behavior was observed on the E1-E5b combination applying Equation (22). Both show that Galileo DGD errors are homogeneous among satel-

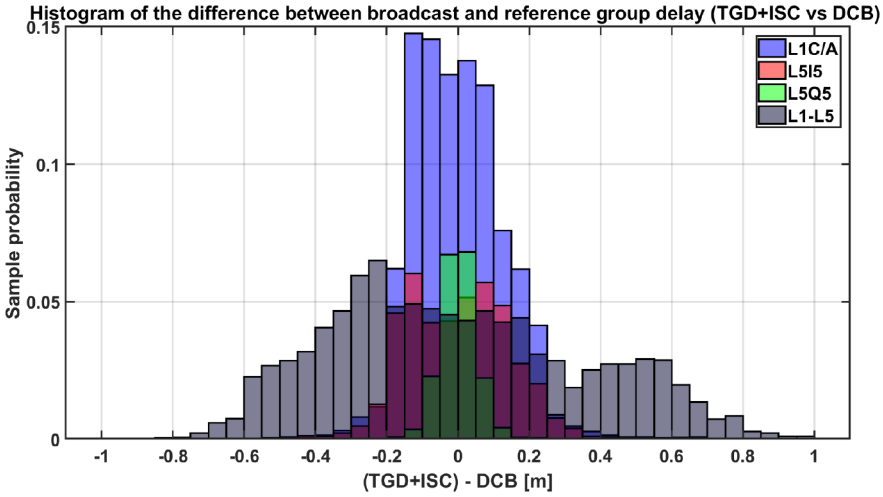

FIGURE 9 Histogram of the GPS GD contributions to the clock error on L1C/A, L5I, L5Q, and L1C/A-L5I combinations [Color figure can be viewed at wileyonlinelibrary.com and www.ion.org]

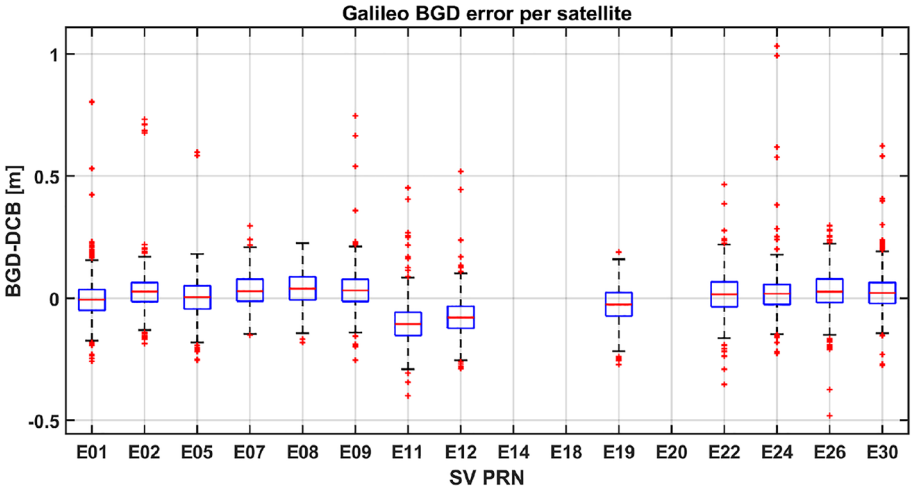

FIGURE 10 Box plot of Galileo broadcast group delay error on E1-E5a. E14 and E18 are the satellites on elliptical orbits for which reference DCB was not available. On each box, the central mark indicates the median, and the bottom and top edges of the box indicate the 25th and 75th percentiles, respectively. The whiskers extend to the most extreme data points not considered outliers, and the outliers are plotted individually using the "+" symbol. The boxplot draws points as outliers if they are greater than $q3 + 2.7\sigma \times (q3 - q1)$ or less than $q1 - 2.7\sigma \times (q3 - q1)$, where $q1$ and $q3$ are the 25th and 75th percentiles of the sample data, respectively, and σ is the sample standard deviation [Color figure can be viewed at wileyonlinelibrary.com and www.ion.org]

lites, and the aggregate histogram is close to a Gaussian distribution.

5 | GALILEO MODEL OF BROADCAST GROUP DELAY BOUNDING

As discussed and shown in the previous sections, this paper exploits the Galileo characteristics to maximize and optimize the performance of ARAIM users.

In the model presented, the bounding of GD errors is separated from the URA. The GD bound is modeled with a new term to be added to the terms of URA. This model exploits the advantage that Galileo DF users are not affected by GD errors: DF users can then apply only URA, which is a tighter bound, not penalized by GD errors as in the GPS case.

The GD bound can then be assumed to be fixed. In fact, the GDs are sufficiently stable over time, and their contributions are expected to be negligible with respect to the ionospheric residual error. The latter shall dominate the SF ranging error budget since its minimum value is 4.5 m.[10] After application of a sufficient safety margin, a fixed value can be assumed.

The model thus offers the following advantages:

- Galileo GD contributions are separated from orbit and clock bounding, and its verification and validation can be simplified in the standardization and certification processes.
- The Galileo URA needs to bound only DF users and does not need to be increased to cover SF users. Reduced bounding values imply improved integrity performance for DF ARAIM users.
- The GD bound can be assessed sporadically, since their values are stable over time. An upper bound can be inserted in the Galileo standard (future versions of the Galileo Open Service-Service Defniniton Documents[16]).
- The GD contribution for SF users is expected to be negligible with respect to the ionospheric error model and can be set to be sufficiently conservative for aviation integrity service.

The next section analyzes and describes the method to combine the GD bound and URA terms.

5.1 | Combination of URA and GD bounding

The correlation and statistical independence of the two components, satellite clock errors and BGD errors, have been analyzed in order to understand the best combination of their bounding. This section examines the correlation between the following two quantities: the error in the estimation of the BGD correction (assessed from Equations (21) and (22)) and the error in the satellite clock offset (assessed with the difference between broadcast clock offsets and reference IGS clock offsets). In particular, the characterization using real data collected between the time of the Galileo Initial Service Declaration in December 2016 and September 2018 was intended to assess whether the generation processes, the observation network, and other architecture elements create dependencies and correlations between the two estimation processes, which prevent separation of the two terms.

TABLE 3 Cross-correlation between Galileo clock and GD errors (01/02/2017-01/09/2018)

Galileo PRN	ρ	P value
E01	0.024840	0.488198
E02	0.000842	0.981256
E05	−0.038575	0.370971
E07	−0.011875	0.783661
E08	−0.020984	0.559690
E09	−0.029483	0.412133
E11	−0.001532	0.965971
E12	−0.001318	0.970729
E19	−0.014597	0.686095
E22	−0.017934	0.658700
E24	−0.018311	0.613544
E26	−0.068680	0.062206
E30	−0.052955	0.143124

Note. P values represent the probabilities of the hypothesis of no correlation.

Figure 12 shows the scatter plot of the BGD error versus the clock offset error for one single Galileo satellite. The fact that no specific pattern can be recognized in the plot is an indication of no correlation between the two estimation errors. The analysis was performed on each satellite individually, and similar results were obtained on the other satellites as confirmed by the cross-correlation results.

The cross-correlation between the two error components (x for satellite clock error and y for GD error) was assessed using the Pearson formula[17]:

$$\rho_{x,y} = \frac{E\left[(x-\mu_x)\left(y-\mu_y\right)\right]}{\sigma_x \sigma_y} \tag{23}$$

where μ_x and μ_y are the mean values for x and y; σ_x and σ_y are the standard deviations for x and y; and $E()$ is the expectation function.

Table 3 shows the correlation results per satellite (second column), which are in absolute value smaller than 1. The third column of the table reports the P values, which are the probabilities of the hypothesis of no correlation: the large P values (bigger than 5%) confirm that the processes are uncorrelated.

These results indicate that these errors can be treated separately and that their bounds can be summed as two independent contributions.

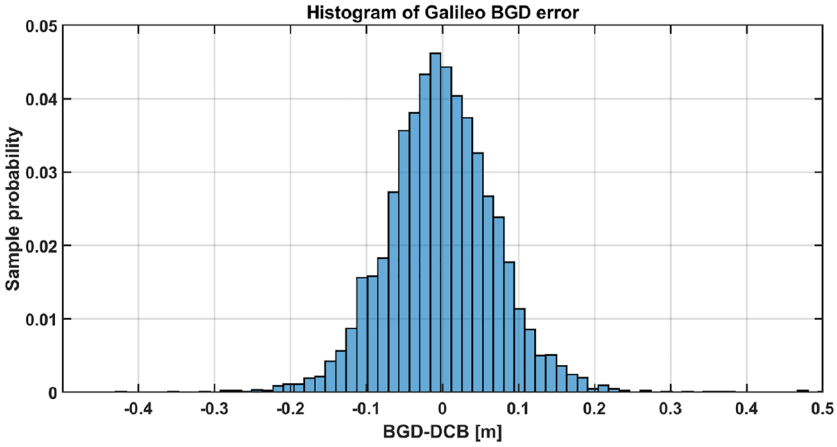

FIGURE 11 Histogram of Galileo broadcast group delay error on E1-E5a [Color figure can be viewed at wileyonlinelibrary.com and www.ion.org]

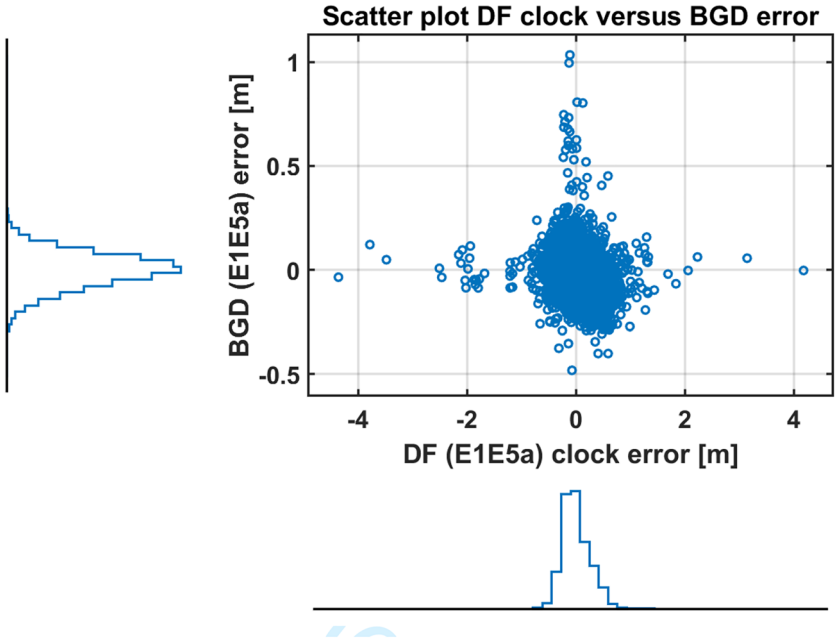

FIGURE 12 Scatter plot of Galileo broadcast group delay errors versus clock errors on E1-E5a for PRN11 (01/02/2017-01/09/2018). Analogous results were obtained for E1-E5b and the other satellites [Color figure can be viewed at wileyonlinelibrary.com and www.ion.org]

For GPS, this contribution is included in the URA value as stated in paragraph 3.3.1.7.2.[12]

The ranging error of an ARAIM user combining the Signal In Space and Integrity Support Message (ISM[8]) would be bounded by a Gaussian distribution with standard deviation obtained from the root sum square of the different error components. In the GPS case, this would correspond to

$$\sigma_i^2 = \sigma_{URA,i}^2 + \sigma_{UIRE,i}^2 + \sigma_{air,i}^2 + \sigma_{tropo,i}^2, \quad (24)$$

where the term $\sigma_{i,URA}$ is the URA broadcast in the GPS Signal In Space. The terms $\sigma_{i,UIRE}$, $\sigma_{i,air}$, and $\sigma_{i,tropo}$ correspond respectively to the ionospheric delay estimation error, the multipath receiver noise, and the tropospheric delay estimation error. These terms are specified in the current GPS MOPS[9] for GPS SF aviation users and can be derived from this standard with proper adjustment to L1-L5 and L5 cases. In particular, $\sigma_{i,air}$ will be different for dual-frequency with respect to SF users. In addition, $\sigma_{i,UIRE}$ represents the ionospheric delay estimation error for the SF case,[9] and in the dual-frequency case, it could be assumed negligible in the absence of scintillation. Note that in the GPS case, the first term $\sigma_{i,URA}^2$ is the same for all services (L1C/A, L5I5, L5Q5, and L1C/A-L5I5).

For Galileo, a dual-frequency user would use the following expression:

$$\sigma_i^2 = \sigma_{URA,i}^2 + \sigma_{UIRE,i}^2 + \sigma_{air,i}^2 + \sigma_{tropo,i}^2, \quad (25)$$

while an SF user would apply the following expression:

$$\sigma_i^2 = \sigma_{URA,i}^2 + \left(\gamma_f \cdot \sigma_{BGD,i}\right)^2 + \sigma_{UIRE,i}^2 + \sigma_{air,i}^2 + \sigma_{tropo,i}^2. \quad (26)$$

The term $\sigma_{i,URA}$ corresponds to the URA broadcast in the Galileo Signal In Space.

The term $\sigma_{i,BGD}$ represents the bound of the GD error, corresponding to a fixed term provided in the Galileo standard.[16]

The term γ_f represents the frequency inflation factor equal to f_{E1}^2/f_{E5a}^2 for E5a users and to 1 for E1 users.

The bounding of the GD error, $\sigma_{i,BGD}$, is assumed to be sufficiently large to also bound in the presence of small biases, such as those shown in Figure 10. Furthermore, it shall ensure that the tail contribution is negligible with respect to the satellite failure probability (P_{sat}) specified in the Galileo standard.[16] For this purpose, the approach applied can be similar to that used in the MOPS DO-229 for the ionosphere bounding: a validation based on real measurement characterization using data recorded at more than 600 worldwide sites during six severe ionospheric storm days in 2003 and 2004.[18] This means that BGD errors might still contain jumps, but the effective impact on the final user would be bounded by $\sigma_{i,BGD}$ and would have a negligible impact on the satellite failure probability with respect to dual-frequency users.

In case the correlation, ρ, between the BGD and URA contributions cannot be considered negligible,

$$\sigma_{URA,SF}^2 = \sigma_{URA,DF}^2 + \sigma_{BGD}^2 + 2\rho \cdot \sigma_{URA,DF} \cdot \sigma_{BGD}, \quad (27)$$

there is an additional term taking into account the cross-correlation and equal to $2\rho \cdot \sigma_{URA,i} \cdot \gamma_f \cdot \sigma_{BGD,i}$ to be included in Equation (26):

$$\begin{aligned}\sigma_i^2 = {} & \sigma_{URA,i}^2 + \left(\gamma_f \cdot \sigma_{BGD,i}\right)^2 \\ & + 2\rho \cdot \sigma_{URA,i} \cdot \gamma_f \cdot \sigma_{BGD,i} + \sigma_{UIRE,i}^2 \\ & + \sigma_{air,i}^2 + \sigma_{tropo,i}^2.\end{aligned} \quad (28)$$

5.2 | Bounds of the Galileo and GPS broadcast group delay errors

This section provides an assessment of the Galileo and GPS GD error-bound term, $\sigma_{i,BGD}$, to be included in future aviation standards.

Figure 13 shows the results of the bounding values based on a Q-Q plot of the DGD errors using measurement data from the characterization described in the previous sections. It is important to mention that two BGD anomalies were observed during the measurement campaign: one on 1/1/2017 and the second one on 06/03/2017. In both cases, satellite E24 transmitted a BGD equal to zero while the true GD was on the order of 12 m. Previously, Galileo satellites in fact used to broadcast BGD equal to zero to indicate a nonvalid value, whenever the BGD could not be computed by the ground system. This procedure has been corrected, and in the future, the satellites will transmit the BGD values from the previous epoch instead of zero values. Consequently, these two anomalies were not included in the statistics used to derive the bounding results representative of future performance expected in 2020.

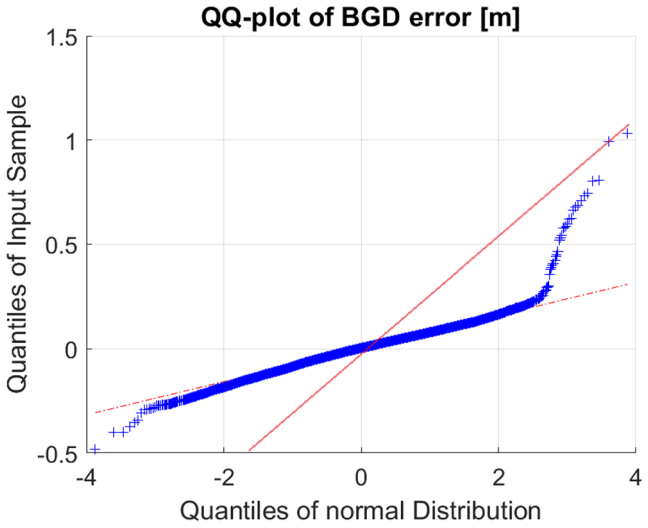

FIGURE 13 Q-Q plot of Galileo group delay errors on E1-E5a [Color figure can be viewed at wileyonlinelibrary.com and www.ion.org]

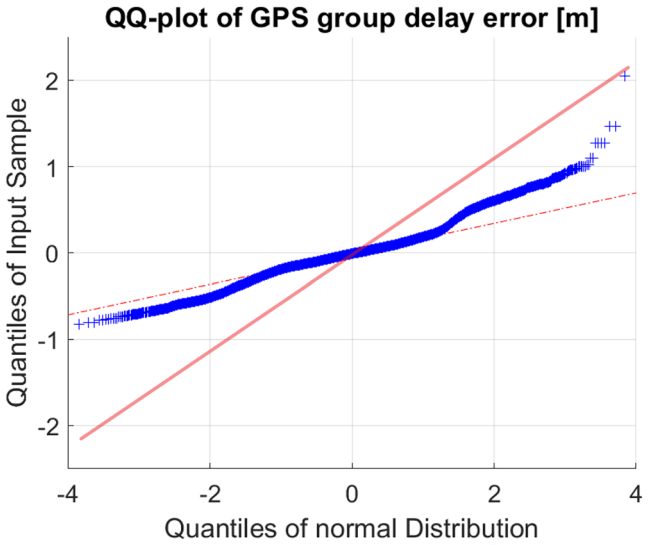

FIGURE 14 Q-Q plot of GPS group delay errors on L1-L5 [Color figure can be viewed at wileyonlinelibrary.com and www.ion.org]

The plot shows a Gaussian distribution in the core of the statistic and the presence of some outliers. The straight line, which bounds the curves, provides an indication of the standard deviation of the Gaussian bounding. In this case, the standard deviation corresponds to the slope of the straight line, that is, around 30 cm.

The analysis of the GD bound described for Galileo was also performed on GPS, and their GD bounding values were compared. The results on GPS, displayed in Figure 14, show and confirm that although GPS and Galileo BGD corrections with similar magnitude, GD bound of the residual errors is larger for GPS (ie, around 50 cm) than for Galileo (ie, around 30 cm), because GPS DF users are penalized

more than Galileo DF (and also SF) users. The reason for this behavior, as described in Section 3.1, is related to the fact that GPS DF users need to apply a larger number of broadcast parameters and their residual errors sum up (see Figure 9). For Galileo, the DF users are not affected, and the SF users are affected only by one single broadcast term.

When using this model in the ARAIM protection level algorithm, the correlation time of the GD errors needs to be assessed and taken into account in the integrity risk assessment. The error correlation time can introduce an additional integrity risk, and the user algorithm needs to design the protection levels to take it into account. An assessment of the GD error correlation time will be part of future work to support the integration of this model in the ARAIM user algorithm.

6 | CONCLUSIONS

Accuracy of GDs and their bounding is essential information in safety critical applications, especially for the high demand integrity service of aviation users.

The GPS standard models this contribution in the URA term, which needs to properly cover the worst case among several GPS services. This corresponds not to the SF service but to the L1-L5 dual-frequency ones, because the GPS navigation message refers to the L1-L2 combination and not to the L1-L5 one.

The Galileo navigation message instead refers directly to the aviation frequencies, L1 and L5, and, consequently, aviation DF users are not affected by GDs. The treatment of their bounding can then be simplified.

The paper presented for Galileo a model of the URA bound separated from the GD one, where the latter needs to be applied only by SF users. The presented model takes advantage of the Galileo signal characteristics and improves integrity availability for DF aviation users. In fact, Galileo URA does not need to be inflated to account for GD errors and refers only to DF services.

A real measurement characterization has shown the motivation and advantages of the presented model. BGD bounds were also assessed to support the definition of future aviation[9] and Galileo standard.[16]

ORCID


Ilaria Martini https://orcid.org/0000-0002-7719-6908

REFERENCES

1. Thoelert S, Enneking C, Vergara M, Sgammini M, Antreich F. GNSS nominal signal distortions—estimation, validation and impact on receiver performance. In: *Proceedings of 28th International Technical Meeting of the Satellite Division of the Institute of Navigation (ION GNSS+2015)*. Tampa, FL; September 2015:1902-1923.
2. Thoelert S, Vergara M, Sgammini M, Antreich F. Estimation of GNSS signal deformation based on measurements with a high gain antenna. In: *Proceedings of the 2014 Space Spectrum Monitoring Conference*; 2014.
3. Okerson G, Ross J, Tetewsky A, Soltz A, Anszperger J, Smith SRJr. Inter-signal correction sensitivity analysis: aperture-dependent delays induced by antenna anisotropy in modernized GPS dual-frequency navigation. *Inside GNSS*. 2016;11(3):44-53.
4. Steigenberger P, Montenbruck O. Galileo status: orbits, clocks, and positioning. *GPS Solutions*. 2017;21(2):319-331.
5. Montenbruck O, Steigenberger P. Differential code bias estimation using multi-GNSS observations and global ionosphere maps. *NAVIGATION*. 2014;61:191-201. https://doi.org/10.1002/navi.64
6. Montenbruck O, Hauschild A. Code biases in multi-GNSS point positioning. In: *Proceedings of the 2013 International Technical Meeting of The Institute of Navigation*. San Diego, CA; January 2013:616-628.
7. Wang N, Yuan Y, Li Z, Montenbruck O, Tan B. Determination of differential code biases with multi-GNSS observations. *J Geod*. 2016;90(3):209-228.
8. Bilateral EU-US Working Group C, ARAIM Technical Subgroup, Milestone 3 Report, February 26, 2016. Annex A. Available at: http://www.gps.gov/policy/cooperation/europe/2016/working-group-c/http://ec.europa.eu/growth/tools-databases/newsroom/cf/itemdetail.cfm?item_id=8690
9. *Minimum Operational Performance Standards for Global Positioning System/Wide Area Augmentation System Airborne Equipment (RTCA/DO-229D MOPS)*; 2006.
10. Perez RO, Prieto-Cerdeira R. Status of NeQuick G after the solar maximum of Cycle 24. *Radio Sci*. 2017;53(3):257-268.
11. Galileo Open Service Interface Control Document, version 1.3. https://www.gsc-europa.eu/system/files/galileo_documents/Galileo-OS-SIS-ICD.pdf; 2016.
12. GPS L1-L2 Interface Control Document. https://www.gps.gov/technical/icwg/IS-GPS-200J.pdf; 2018.
13. GPS L5 Interface Control Document. https://www.gps.gov/technical/icwg/IS-GPS-705E.pdf; 2018.
14. Receiver Independent Navigation Exchange Format, Version 3.03. ftp://igs.org/pub/data/format/rinex303.pdf; 2015.
15. The IGS Multi-GNSS Experiment and Pilot Project (MGEX). http://mgex.igs.org/; 2012.
16. Galileo Open Service—Service Definition Document. https://www.gsc-europa.eu/system/files/documents/Galileo-OS-SDD.pdf; 2019.
17. Rogers JL, Nicewander WA. Thirteen ways to look at the correlation coefficient. *Amer Statist*. 1988;42(1):59-66.
18. El-Arini MB, Conker R, Lejeune R, Fernow JP, Hsiao T. Validation of the en route through NPA GPS Ionospheric Delay Model in the WAAS MOPS (DO-229C). TCA Special Committee 159, Working Group 2; 2005.

How to cite this article: Martini I, Sgammini M, Pablo Boyero J. Galileo model of group delay accuracy for advanced RAIM users. *NAVIGATION*. 2020;67:129–141. https://doi.org/10.1002/navi.356